Cohesive Properties of Ionic Liquids Calculated from First Principles

Supporting Information

Ctirad Červinka[*]*, Martin Klajmon, Vojtěch Štejfa*

[†] Department of Physical Chemistry, University of Chemistry and Technology Prague, Technická 5, CZ-166 28 Prague 6, Czech Republic

*****Corresponding author: cervinkc@vscht.cz

S1. Reference experimental data

Reported information on water content does not often correlate with T_{fus}. For example, Nishida et al. [1] report a very low water content for $[C_1C_2Im][BF_4]$, but their T_{fus} is rather lower compared to the rest of literature data and a pronounced peak well below T_{fus} can be seen in the thermogram presented in ref. [1] (but not reported elsewhere), which undoubtedly corresponds to the eutectic temperature. Weighted averages presented in Table S1 were calculated from the bold values considered as more reliable based on following factors: presented uncertainty, reported calibration procedure, and availability of the $\Delta_{fus}H$.

TABLE S1
Fusion temperatures T_{fus} and enthalpies $\Delta^{l}_{cr}H_m$ reported in the literature.

Reference [a]	T_{fus} / K	$\Delta^{l}_{cr}H_m$ / kJ mol^{-1}	Water content [b]	Method
		$[C_1C_2Im][NTf_2]$, crI		
Paulechka et al. 2007 [2]	**271.44 ± 0.03**	**21.89 ± 0.03**	**<0.016**	**Adiabatic calorimetry**
		$[C_1C_2Im][BF_4]$		
Mutch and Wilkes, 1998 [3]	277.6 ± 0.5	22 ± 2	NA	DSC
Holbrey and Seddon, 1999 [4]	279.0	**10.1**	**<200 ppm**	**DSC**
Ngo et al. 2000 [5]	284	NA	<20 ppm	DSC
Noda et al. 2001 [6]	288	NA	vacuum-dried	DSC
Nishida et al. 2003 [1]	**286**	**NA**	**<50 ppm**	**DSC**
Van Valkenburg et al. 2005 [7]	**287.6 ± 0.4**	**9.5 ± 0.4**	**650 ppm**	**DSC**
Wachter et al. 2010 [8]	**286.6 ± 0.2**	**NA**	**21 ppm**	**heating curve**
Wachter et al. 2010 [8]	**286.975 ± 0.007**	**NA**	**21 ppm**	**conductivity**
Shirota et al. 2011 [9]	**287.8 ± 0.7**	**NA**	**<256 ppm**	**DSC**
Vila et al. 2012 [10]	288	NA	<1000 ppm	conductivity

Weighted average [c]	**287.0 ± 0.7**	**9.6 ± 0.5**		
		$[C_1C_2Im][PF_6]$, crI		
Ngo et al. 2000 [5]	335	NA	<20 ppm	DSC
Wong et al. 2002 [11]	334	NA	"0"	DSC
Dzyuba and Bartsch 2002[12]	331	7.1	NA	DSC
Domanska and Marciniak 2003[13]	**332.80**	**17.86**	**NA**	**DSC**
Sifaoui et al. 2007[14]	**334.0 ± 0.3**	**17.9 ± 0.1**	**NA**	**DSC**
Vila et al. 2012 [10]	333	NA	149.7 ppm	conductivity
Endo et al. 2013 [15]	336	19.0	NA	Custom-built calorimeter
Serra et al. 2017[16]	**334.2 ± 0.3**	**17.7 ± 0.1**	**<500 ppm**	**DSC**
Weighted average [c]	**334.1 ± 0.3**	**17.8 ± 0.3**		

[a] References in bold were accepted for the correlation.
[b] Mass fraction of water determined by Karl-Fischer titration is specified except for ref.[2], where overall purity was determined from a fractional-melting experiment.
[c] Presented uncertainties of the average are estimated to follow reliability of the values.

Although the uncertainty of the heat capacity from adiabatic measurements is not reported in the original work,[2] an expanded uncertainty $0.004\,C_p$ has been assigned to the same calorimeter recently.[17] Other literature studies for $[C_1C_2Im][NTf_2]$ are omitted except for the one by Ferreira et al.[18] because of the overlapping temperature range and inferior uncertainty compared to adiabatic calorimetry. Note that although the authors[18] state that DSC and their modulated variants have uncertainty of at least 5%, they incomprehensibly state an unrealistically low uncertainty for their measurements.

TABLE S2
Condensed phase heat capacities $C_{p,m}$ reported in the literature.

Reference [a]	N [b]	T range / K	$u(C_{p,m})$ [c]	Method [d]
		$[C_1C_2Im][NTf_2]$, crI		
Paulechka et al. 2007[2]	**34**	**0 – 271**	NA	**Adiabatic calorimetry**
		$[C_1C_2Im][NTf_2]$, l		
Paulechka et al. 2007 [2]	**16**	**257 – 370**	NA	**Adiabatic calorimetry**
Ferreira et al. 2012 [18]	**75**	**343 – 463**	<1.2 J K^{-1} mol^{-1}	HF-DSC (M)
		$[C_1C_2Im][BF_4]$, l		
Sanmamed et al. 2010 [19]	**9**	**283 – 323**	**0.002** $C_{p,m}$	**TC-DSC**
Gupta et al. 2016 [20]	**4**	**293 – 308**	**0.008** $C_{p,m}$	**TC-DSC**
Mutch and Wilkes 1998 [3]	12	283 – 403		HF-DSC (M)
Sharma et al. 2013 [21]	**4**	**293 – 308**	**0.003** $C_{p,m}$	**TC-DSC**
Van Valkenburg et al. 2005 [7]	S	273 – 403	NA	HF-DSC (M)
Waliszewski et al. 2005 [22]	**16**	**283 – 358**	**0.0015** $C_{p,m}$	**TC-DSC**
Yu et al. 2009 [23]	12	303 – 358	4 J K^{-1} mol^{-1}	HF-DSC
		$[C_1C_2Im][PF_6]$, crI		
Serra et al. 2017[16]	**5**	**280 – 300**	**0.005** $C_{p,m}$	**TC-DSC**
		$[C_1C_2Im][PF_6]$, l		
Holbrey et al. 2003[24]	11	353 – 453	NA	HF-DSC (M)
Serra et al. 2017[16]	**4**	**340 – 355**	**0.005** $C_{p,m}$	**TC-DSC**

[a] References in bold were accepted for the correlation..
[b] Number of presented heat capacity data points. S stands for smoothed data.
[c] Presented standard uncertainties of the $C_{p,m}$ measurements.
[d] Used shortcuts are: TC: Tian-Calvet, HF: heat flux, M: modulated run.

Various methods are commonly employed for determination of volatility of ILs that can be classified according to the obtained primary data closely connected to the evaporation regime: i) direct determination of vaporization enthalpy $\Delta_{vap}H$, ii) determination of equilibrium

evaporation rate or vapor pressures (related to $\Delta_{vap}H$ through temperature dependence), and iii) determination of evaporation rate to vacuum (related to internal energy of vaporization $\Delta_{vap}U$). The evaporation rate is further quantified either gravimetrically, by deposition onto quartz crystal microbalance (QCM), using vapor-phase mass spectra (MS), or by a suspension balance. Less common are determinations of evaporation rate through magnetic suspension balance, commercial thermogravimetric analysis (TGA), or calorimetric heat capacity of the sample.

TABLE S3
Experimental studies of vapor pressures and vaporization enthalpies.

Reference [a]	N [b]	T range / K	$\Delta_l^g H_m(\overline{T})$ / kJ mol^{-1}	Method [c]
		$[C_1C_2Im][NTf_2]$		
Zaitsau et al. 2006 [25]	**7**	**442 – 484**	118.8 ± 1.3	**Knudsen Effusion**
Armstrong et al. 2007 [26]	H	300 – 550	121.6 ± 1.9	TPD + MS
Emel'yanenko et al. 2007 [27]	**7**	**499 – 538**	NA	**Transpiration**
Tolstoguzov 2007 [28] (as in [29])	H	400 – 560	130 ± 10	Knudsen effusion + MS
Santos et al. 2007 [30]	**H**	**577.8**	**110.4 ± 2.4**	**Vaporization calorimetry**
Luo et al. 2008 [31]	H	473 – 518	118.5 ± 0.4	TGA
Lovelock et al. 2010 [32]	S	359 – 436	122	TPD + MS
Wang, et al. 2010 [33]	H	T_{avg} = 573	111.7 ± 1.7	Knudsen effusion + UV
Rocha et al. 2011 [34]	**20**	**445 – 483**	114.6 ± 0.5	**Knudsen effusion + QCM**
Verevkin et al. 2011 [35], Zaitsau et al. 2012 [36], Verevkin et al. 2013 [37]	**H**	**362 – 395**	**118.6 ± 1.0**	**TPD + QCM**
Verevkin et al. 2012 [38], Verevkin et al. 2013 [37]	**H**	**480 – 570**	**110.5 ± 1.5**	**TGA**
Ahrenberg et al. 2014 [29]	**H**	**500 – 750**	**108.2 ± 1.9; 110 ± 1.2**	**ultra-fast scanning calorimetry**

Heym et al. 2015 [39]	38	538 – 723	NA	horizontal thermobalance TGA
Heym et al. 2015 [39]	23	363 – 473	NA	Magnetic suspension balance TGA
Ahrenberg et al. 2016 [40]	1	**358 – 373**	**199.2 ± 4**	**AC calorimetry**
Dunaev et al. 2016 [41]	H	422 – 520	117 ± 2	Knudsen Effusion + MS
Santos et al. 2018 [42]	**65**	**433 – 503**	115.0 ± 0.4; 115.3 ± 0.3	**Knudsen effusion + QCM**
		$[C_1C_2Im][BF_4]$		
Deyko et al. 2009 [43]	H	T_{avg} = 515	128 ± 2	TPD + MS
Zaitsau et al. 2012 [36]	**H**	**411 - 454**	**122.2 ± 1.0**	**TPD + QCM**
		$[C_1C_2Im][PF_6]$		
Zaitsau et al. 2012 [36]	**H**	**414-457**	**129.9 ± 1.0**	**TPD + QCM**

[a] References in bold were accepted for the correlation. If several vapor pressure values were available, vaporization enthalpy was not correlated separately not to duplicate the inputs.
[b] Number of presented vapor pressure data points. S stands for smoothed data; H is listed, where only the vaporization enthalpy was presented.
[c] Used shortcuts are: TPD: temperature programmed desorption, MS: mass spectrometry, QCM quartz crystal microbalance, TGA: thermogravimetric analysis, MS: mass spectra.

S2. Simultaneous correlation procedure and thermodynamic relationships between the experimental data

Simultaneous correlation of vapor pressures and related thermal properties (SimCor) was suggested (in a simplified form) by King and Al-Najjar in 1974.[44-45] The method was later sporadically used by several authors (e.g. by Wexler,[46] Ambrose and Davies,[47] Mosselman et al.,[48] Rogalski,[49] King and Mahmud,[50] Craven and de Reuck,[51] Poling,[52] Varushchenko et al.,[53] Huber et al.,[54] and Hogge et al.[55-56]) and systematically in our laboratory.[57-65] The SimCor method is based on exact thermodynamic relationships and the procedure must, therefore, yield reliable results provided that the input data are of reasonable accuracy. A great advantage of this approach is that a single vapor pressure equation can furnish a description of the temperature dependences of several thermodynamic properties and the SimCor thus also provides a test on the consistency of different experimental data.

According to the Clapeyron equation, the vaporization enthalpy $\Delta_{vap}H$ is related to temperature dependence of vapor pressure:

$$R\left(\mathrm{d}\ln p / \mathrm{d}(1/T)\right)_{sat} = \Delta_{vap}H / \Delta_{vap}z\,, \qquad \textbf{(S.1)}$$

where $\Delta_{vap}z$ is the difference between the compressibility factors of the coexisting liquid and gas phases. If we restrict the calculations to region of low vapor pressures (i.e. below 1 kPa, which is justifiable for the purposes of this work), we can use the ideal-gas equation for evaluation of compressibility factor of the gas phase and neglect the compressibility factor of the liquid phase. The equation (S.1) simplifies to

$$R\left(\mathrm{d}\ln p / \mathrm{d}(1/T)\right)_{sat} = \Delta_{vap}H\,. \qquad \textbf{(S.2)}$$

When describing the vapor pressure using the Clarke and Glew equation (equation (4) in the main text), one obtains a logical relationship for calculating $\Delta_{vap}H(T)$ using the adjustable parameters of the vapor pressure equation:

$$\Delta_{vap}H(T) = \Delta_{vap}H^{0}(\theta) + (T-\theta)\Delta_{vap}C_p^{0}(\theta) + \frac{(T-\theta)^2}{2}\frac{\partial\Delta_{vap}C_p^{0}}{\partial T}(\theta)\,, \qquad \textbf{(S.3)}$$

where θ is a selected reference temperature and $\Delta_{vap}C_p^{0}(\theta)$ is the difference between the heat capacity of liquid and ideal-gas phase. Since $\Delta_{vap}C_p(T) = C_p^{g} - C_p^{l}$ is physically a derivative of $\Delta_{vap}H(T)$ with respect to temperature, one can easily obtain the linear relationship

$$\Delta_{vap}C_p(T) = \Delta_{vap}C_p^{0}(\theta) + (T-\theta)\frac{\partial\Delta_{vap}C_p^{0}}{\partial T}(\theta)\,. \qquad \textbf{(S.4)}$$

Thus, parameters of the vapor pressure equation can be used to calculate several thermodynamic quantities: $p(T)$, $\Delta_{vap}H(T)$, and $\Delta_{vap}C_p(T)$. If an appropriate objective function S is selected, one can minimize error in description of multiple types of experimental data in one procedure. The objective function S is here defined as

$$S = \sum_{i=1}^{m_p} \frac{\left(\ln p^{\mathrm{exp}} - \ln p^{\mathrm{calc}}\right)_i^2}{\sigma_i^2(\ln p)} + \sum_{i=1}^{m_H} \frac{\left(\Delta_{\mathrm{vap}} H^{\mathrm{exp}} - \Delta_{\mathrm{vap}} H^{\mathrm{calc}}\right)_i^2}{\sigma_i^2(\Delta_{\mathrm{vap}} H)} + \sum_{i=1}^{m_C} \frac{\left(\Delta_{\mathrm{vap}} C_p^{\mathrm{exp}} - \Delta_{\mathrm{vap}} C_p^{\mathrm{calc}}\right)_i^2}{\sigma_i^2(\Delta_{\mathrm{vap}} C_p)}, \quad \textbf{(S.5)}$$

where the quantities with the superscript "exp" relate to the experimental data ($\Delta_{\mathrm{vap}} C_p^{\mathrm{exp}}$ are calculated from experimental C_p^{l} data points and theoretically calculated C_p^{g} fitted by a polynomial function to provide C_p^{g} at the temperatures of determination of C_p^{l} data) and the quantities with the superscript "calc" are expressed from the vapor pressure equation according to equations (4) in the main text, (S.3), and (S.5). The individual data points are weighted using their expected uncertainties σ_i. As a starting point, uncertainties claimed in the original data source are used, but are raised during the evaluation when inconsistency with other types of data is observed. If no experimental vapor pressure data is available, one can use the objective function with the first term equal to zero and obtain all adjustable parameters but $\Delta_{\mathrm{vap}} G^0$.

Finally, sublimation enthalpy at the temperature of fusion $\Delta_{\mathrm{sub}} H\,(T_{\mathrm{fus}})$ can be calculated as

$$\Delta_{\mathrm{sub}} H\,(T_{\mathrm{fus}}) = \Delta_{\mathrm{vap}} H\,(T_{\mathrm{fus}}) + \Delta_{\mathrm{fus}} H\,(T_{\mathrm{fus}}) \quad \textbf{(S.6)}$$

using averages of experimental values for $\Delta_{\mathrm{fus}} H$ and T_{fus} and $\Delta_{\mathrm{vap}} H\,(T_{\mathrm{fus}})$ calculated from equation (S.4).

S3. Temperature dependence of vaporization enthalpies

Since the very first measurements of $\Delta_{vap}H$ of $[C_1C_2Im][NTf_2]$, the authors were suggesting different values of $\Delta_{vap}C_p$ for recalculation to 298 K. $\Delta_{vap}C_p$(298 K) = −100 $J \cdot K^{-1} \cdot mol^{-1}$ was used for various alkylmethylimidazolium ILs in refs.[25, 27] derived from $\Delta_{vap}C_p$(298 K) = −105 $J \cdot K^{-1} \cdot mol^{-1}$ calculated for $[C_4C_1Im][PF_6]$ based on calorimetric data and statistical thermodynamics. This value was later recommended (probably due to lack of any other data) as applicable for all members of the $[C_nC_1Im][NTf_2]$ family and generally for any ionic liquids.[66] Another close value of −94 $J \cdot K^{-1} \cdot mol^{-1}$ is used in ref. [26, 32], which was calculated originally for $[C_4C_1Im][NTf_2]$ at 323 K based on the energy equipartition principle.[67] Santos et al. [30]estimated $\Delta_{vap}C_p$ = −90.7 $J \cdot K^{-1} \cdot mol^{-1}$ (as an average value over a temperature range 298.15 to 577.8 K) based on the energy equipartition principle. Rocha et al.[34] used $\Delta_{vap}C_p$(388 K) = −112 $J \cdot K^{-1} \cdot mol^{-1}$ based on calorimetric and statistical thermodynamics data for the discussed compound. The probably last approach used by Verevkin and coworkers[37, 40] is based on difference between $\Delta_{vap}H$ obtained over two temperature ranges, yielding in values −56 and −53 $J \cdot K^{-1} \cdot mol^{-1}$ (for temperature range 380 to 572 K and 358 to 780 K, respectively), denoted incorrectly as $\Delta_{vap}C_p$(298 K).

To sum up, four approaches for evaluation of $\Delta_{vap}C_p$ were used, each suffering from specific inaccuracies: i) transfer from different IL, ii) estimation based on energy equipartition principle, iii) temperature dependence of experimental $\Delta_{vap}H$, and most reliable iv) combination of calorimetric data and statistical thermodynamics. One deficiency is however common for all four approaches, neglecting of temperature dependence of the $\Delta_{vap}C_p$ term. Correlation used in this work assumes a linear dependence of $\Delta_{vap}C_p$, as shown in Figure 3 in the main text. Most of the discussed estimations are in an acceptable agreement with the SimCor results, if they were considered at adequate temperatures, but none of them is actually adequate for correcting the $\Delta_{vap}H$ to 298 K because of the neglected temperature dependence.

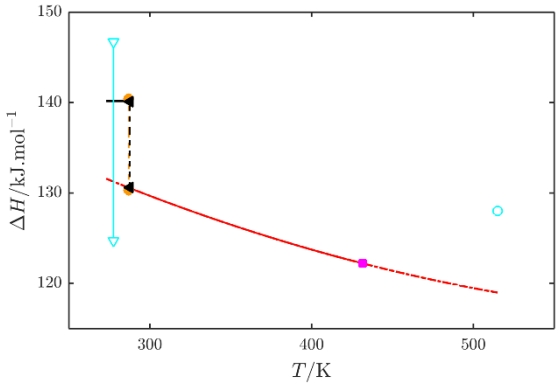

FIGURE S1. Experimental reference data on $\Delta_{vap}H$ and $\Delta_{fus}H$ (illustrated by the vertical lines at the temperatures of the melting point) for [C_1C_2Im][BF_4] along with the temperature dependence of $\Delta_{vap}H$ obtained by the SimCor method (red line). $\Delta_{vap}H$ sources: ○, Deyko et al.[43]; ■, Zaitsau et al.[36] $\Delta_{fus}H$ sources: ▽, Mutch and Wilkes[3]; ●, Holbrey and Seddon[4]; ◀, Van Valkenburg et al.[7] Data sets given with empty symbols were excluded from the SimCor correlations.

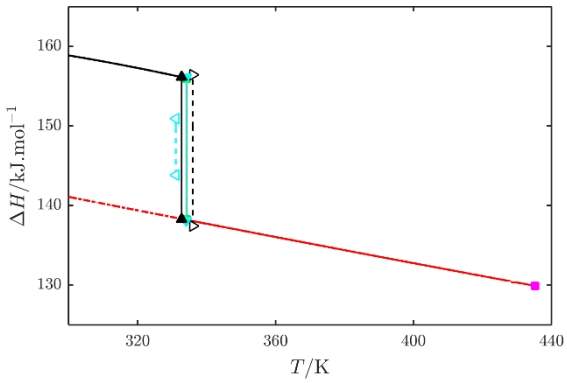

FIGURE S2. Experimental reference data on $\Delta_{vap}H$ and $\Delta_{fus}H$ (illustrated by the vertical lines at the temperatures of the melting point) for [C_1C_2Im][PF_6] along with the temperature dependence of $\Delta_{vap}H$ obtained by the SimCor method (red line). $\Delta_{vap}H$ sources: ■, Zaitsau et al.[36] $\Delta_{fus}H$ sources: ◁, Dzyuba and Bartsch[12]; ▲, Domanska and Marciniak[13]; ▼, Sifaoui et al.[14]; ▷, Endo et al. [15]; ■, Serra et al.[16]. Data sets given with empty symbols were excluded from the SimCor correlations.

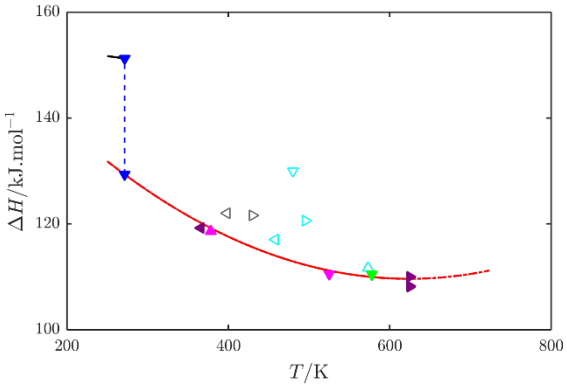

FIGURE S3. Experimental reference data on $\Delta_{vap}H$ and $\Delta_{fus}H$ (illustrated by the vertical lines at the temperatures of the melting point) for $[C_1C_2Im][NTf_2]$ along with the temperature dependence of $\Delta_{vap}H$ obtained by the SimCor method (red line). $\Delta_{vap}H$ sources: ▼, Santos et al.[30], ▷, Armstrong et al.[26], ▽, Tolstoguzov[28], ▷, Luo et al.[31], △, Wang, et al.[33], ◁, Lovelock et al.[32], ▲, Verevkin et al.[35], ▼, Verevkin et al.[38], ▶, Ahrenberg et al.[29], ◀, Ahrenberg et al.[40], ◁, Dunaev et al.[41] $\Delta_{fus}H$ sources: ▼, Paulechka et al.[2] Data sets given with empty symbols were excluded from the SimCor correlations.

S4. Calculated properties of ideal-gaseous ILs

TABLE S4

Isobaric heat capacities ($J \cdot K^{-1} \cdot mol^{-1}$) of investigated ILs and bare ions in the ideal-gaseous state as a function of temperature calculated from optimized ionic geometries, and other molecular parameters obtained at the PBE-D3(BJ)/6-311+G(d,p) level.

	[emIm]	[BF_4]	[PF_6]	[NTf_2]	[emIm][BF_4]		[emIm][PF_6]		[emIm][NTf_2]	
T / K	$C_{p,\mathrm{ion}}^{g0}$ [a]	$C_{p,\mathrm{ion}}^{g0}$ [a]	$C_{p,\mathrm{ion}}^{g0}$ [a]	$C_{p,\mathrm{ion}}^{g0}$ [a]	C_{inter}^{g0}	$C_{p,\mathrm{pair}}^{g0}$ [b]	C_{inter}^{g0}	$C_{p,\mathrm{pair}}^{g0}$ [b]	C_{inter}^{g0}	$C_{p,\mathrm{pair}}^{g0}$ [b]
25	41.42	33.26	33.26	59.55	39.50	80.92	19.06	60.51	21.66	89.40
50	53.00	33.39	33.87	76.41	62.52	115.65	40.85	94.46	37.65	133.80
75	61.55	34.74	37.67	96.31	73.55	136.58	58.03	124.08	49.11	173.79
100	69.05	37.94	44.97	117.36	76.15	149.88	67.50	148.26	57.04	210.18
125	75.83	42.48	54.84	137.09	73.11	157.51	69.46	165.17	62.24	241.68
150	83.21	47.08	64.56	154.87	68.54	165.57	65.37	179.88	65.55	270.37
175	90.85	51.87	74.72	170.40	65.40	175.29	58.98	191.87	67.46	295.18
200	99.31	56.35	83.80	184.60	63.71	186.11	53.24	203.09	68.46	319.10
225	108.53	60.47	91.76	197.37	62.31	198.04	50.02	217.74	68.98	341.91
250	117.95	64.53	99.53	208.66	61.60	210.82	47.52	231.74	69.23	362.57
275	128.07	68.10	105.82	219.31	61.23	223.78	45.22	245.10	69.45	383.86
300	138.35	71.48	111.60	228.80	60.64	237.21	43.16	259.85	69.84	403.73
325	148.67	74.60	116.78	237.52	60.26	250.54	41.49	273.61	70.36	423.01
350	159.26	77.26	120.71	245.86	60.32	263.58	40.12	286.83	71.08	442.95
375	169.54	79.78	124.48	253.28	60.41	276.34	39.07	300.26	71.98	461.34
400	179.63	82.00	127.61	260.27	60.05	288.42	38.24	312.22	72.89	479.53

[a] Estimated standard uncertainty is 2%.
[b] Estimated standard uncertainty is 3%.

TABLE S5

Entropies ($J \cdot K^{-1} \cdot mol^{-1}$) of investigated ideal-gaseous ILs at 100 kPa as a function of temperature calculated from optimized ionic geometries, and other molecular parameters obtained at the PBE-D3(BJ)/6-311+G(d,p) level.

	[emIm][BF_4]	[emIm][PF_6]	[emIm][NTf_2]
T / K	S^{g0} [a]	S^{g0} [a]	S^{g0} [a]
25	254.05	246.68	284.38
50	321.83	299.29	360.50
75	373.03	343.34	422.41
100	414.31	382.49	477.49
125	448.74	417.63	527.91
150	478.27	449.22	574.61
175	504.40	477.81	618.22
200	528.45	504.09	659.25
225	551.06	528.84	698.12
250	572.59	552.49	735.19
275	593.30	575.24	770.72
300	613.35	597.24	804.95
325	632.86	618.58	838.06
350	651.91	639.34	870.16
375	670.53	659.57	901.36
400	688.75	679.32	931.73

[a] Estimated standard uncertainty is 3%.

S5. Calculated properties of crystalline ILs

TABLE S6
Statistic of the dispersion corrections of the MP2C method evaluated for the three investigated ILs at the HMBI MP2C-F12/avdz+pB3LYP level of theory.

	[emIm][BF_4]	[emIm][PF_6]	[emIm][NTf_2]
Pair interactions within 10 Å	175	167	143
Fraction of positive dispersion corrections	63%	69%	94%
Mean value of the correction (kJ·mol^{-1})	0.06	0.04	0.17
Mean absolute value of the correction (kJ·mol^{-1})	0.10	0.07	0.18
Mean absolute percentage value of the correction	0.05%	0.03%	0.08%

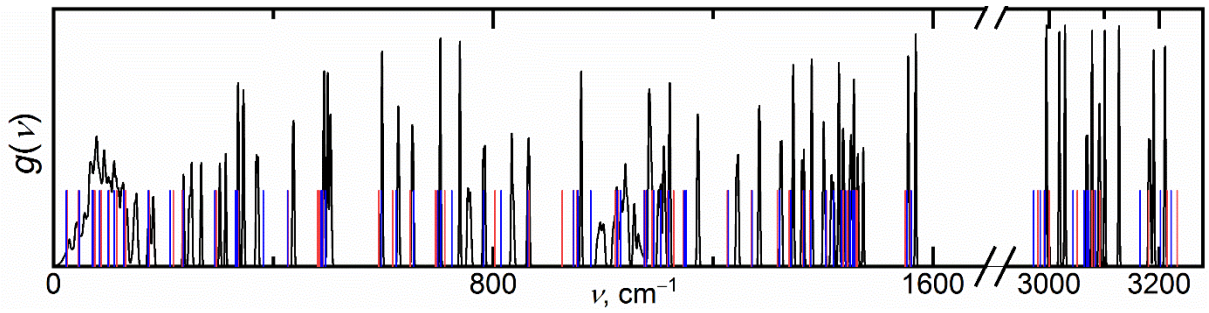

FIGURE S4. Calculated density of phonon states $g(\nu)$ for crystalline [emIm][BF_4] (black) compared with the fundamental vibrational frequencies of an isolated [emIm][BF_4] ion pair in the most stable conformation (relative intensities discarded), all obtained at the PBE-D3(BJ) level of theory. Red and blue lines mark the values obtained using the split-valence 6-311+G(d,p) basis set in Gaussian and the PAW framework in VASP, respectively.

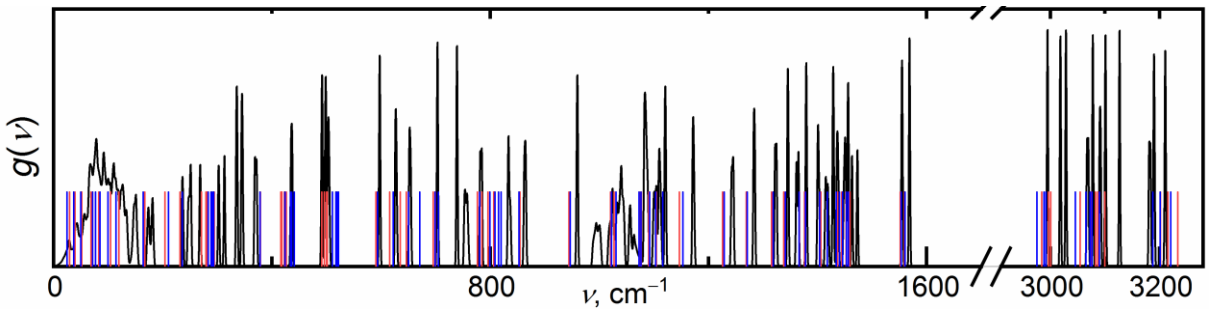

FIGURE S5. Calculated density of phonon states $g(\nu)$ for crystalline [emIm][PF_6] (black) compared with the fundamental vibrational frequencies of an isolated [emIm][PF_6] ion pair in the most stable conformation (red, relative intensities discarded), both obtained at the PBE-D3(BJ) level of theory.

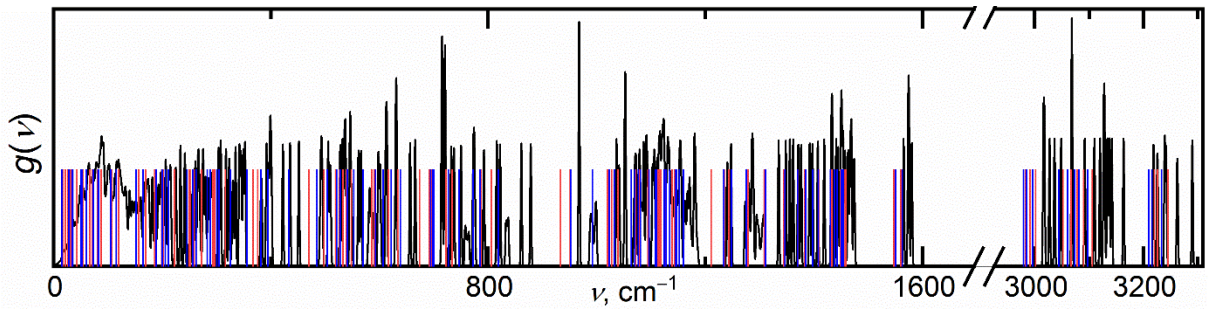

FIGURE S6. Calculated density of phonon states $g(\nu)$ for crystalline [emIm][NTf_2] (black) compared with the fundamental vibrational frequencies of an isolated [emIm][NTf_2] ion pair in the most stable conformation (red, relative intensities discarded), both obtained at the PBE-D3(BJ) level of theory.

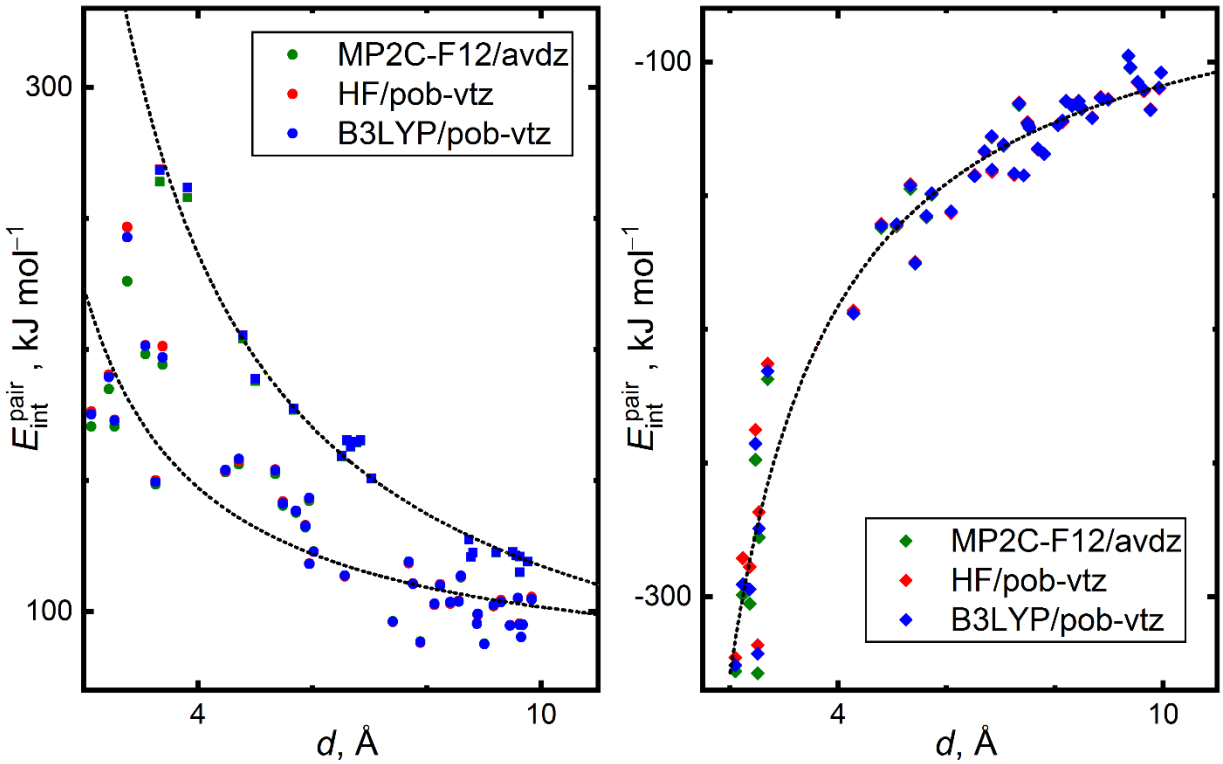

FIGURE S7. Pair interaction energies of the proximate ion pairs from the optimized [emIm][BF_4] crystal lattice as a function of the closest contact distance of the ions. Squares, circles and diamonds correspond to interactions anion-anion, cation-cation and cation-anion, respectively. Hyperbolic fits are drawn to guide the eye.

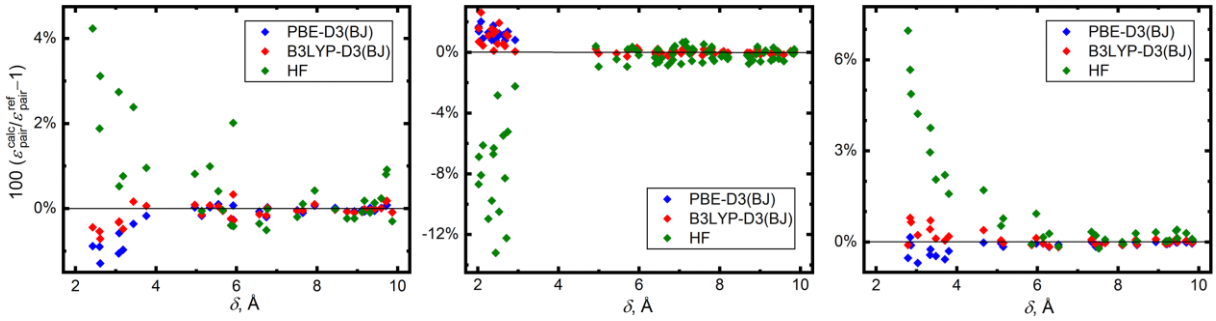

FIGURE S8. Percentage deviation of the pair interaction energies of the proximate ion pairs from the optimized [emIm][NTf_2] crystal lattice as a function of the closest contact distance of the ions. MP2C-F12/aug-cc-pVDZ level of theory is the reference for anion-anion and cation-anion interactions. Left – interactions cation-cation, middle – cation-anion, right anion-anion.

TABLE S7

Molar volume ($cm^3 \cdot mol^{-1}$) of investigated crystalline ILs at zero pressure as a function of temperature calculated from optimized unit-cell geometries and phonons obtained at the PBE-D3(BJ)/PAW(400 eV) level and unit-cell energy – volume profiles refined either at the B3LYP-D3(BJ)/PAW(1000 eV) or HMBI MP2C-F12/avdz+pB3LYP levels of theory.

	[emIm][BF_4]			[emIm][PF_6]			[emIm][NTf_2]		
T / K	PBE	B3LYP	HMBI	PBE	B3LYP	HMBI	PBE	B3LYP	HMBI
0	140.80	132.13	131.03	156.77	145.81	148.02	247.08	223.98	225.90
50	141.51	132.53	131.44	156.87	145.95	148.11	247.92	224.18	226.34
100	142.95	133.53	132.52	157.06	146.47	148.48	250.00	224.78	227.68
150	144.70	134.78	133.94	157.43	147.11	148.96	252.17	225.52	229.46
200	146.78	136.22	135.64	157.87	147.79	149.47	254.20	226.32	231.54
250	149.26	137.84	137.64	158.35	148.48	149.99	256.03	227.16	233.89
300	152.25	139.65	139.99	158.84	149.17	150.51	257.66	228.03	236.46
350	155.84	141.67	142.75	159.33	149.85	151.03	259.09	228.91	239.19
400	160.06	143.91	145.97	159.81	150.52	151.54	260.36	229.81	242.00

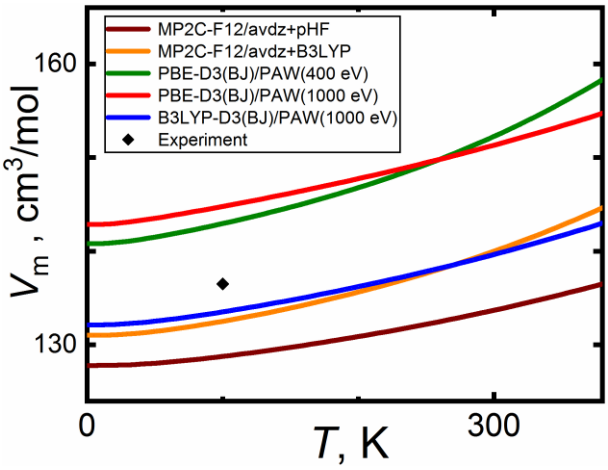

FIGURE S9. Molar volume of crystalline [emIm][BF_4] calculated from optimized unit-cell geometries and phonons obtained at the PBE-D3(BJ)/PAW(400 eV) level and unit-cell energy – volume profiles refined at various levels of theory.

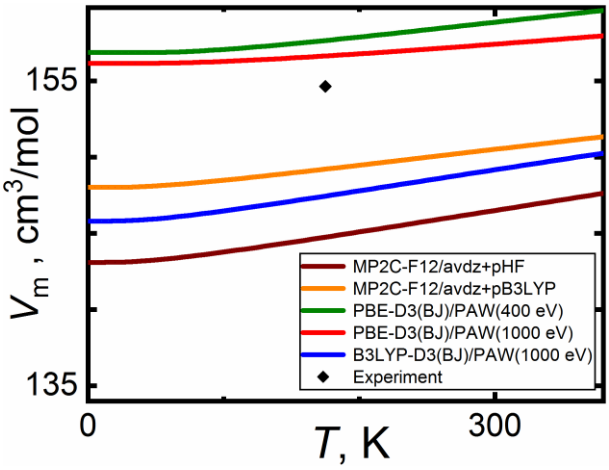

FIGURE S10. Molar volume of crystalline [emIm][PF_6] calculated from optimized unit-cell geometries and phonons obtained at the PBE-D3(BJ)/PAW(400 eV) level and unit-cell energy – volume profiles refined at various levels of theory.

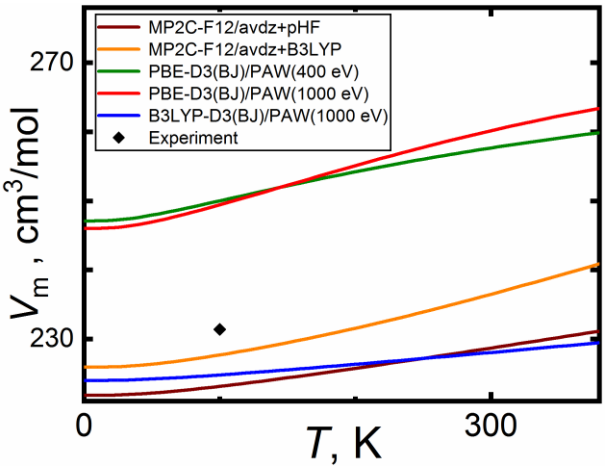

FIGURE S11. Molar volume of crystalline [emIm][NTf_2] calculated from optimized unit-cell geometries and phonons obtained at the PBE-D3(BJ)/PAW(400 eV) level and unit-cell energy – volume profiles refined at various levels of theory.

TABLE S8

Isobaric heat capacities ($J \cdot K^{-1} \cdot mol^{-1}$) of investigated crystalline ILs as a function of temperature calculated from optimized unit-cell geometries and phonons obtained at the PBE-D3(BJ)/PAW(400 eV) level and unit-cell energy – volume profiles refined either at the B3LYP-D3(BJ)/PAW(1000 eV) or HMBI MP2C-F12/avdz+pB3LYP levels of theory.

	[emIm][BF_4]			[emIm][PF_6]			[emIm][NTf_2]		
T / K	PBE	B3LYP	HMBI	PBE	B3LYP	HMBI	PBE	B3LYP	HMBI
0	0.00	0.00	0.00	0.00	0.00	0.00	0.00	0.00	0.00
50	79.18	72.27	71.38	82.80	77.09	78.46	125.65	110.77	112.60
100	128.41	124.58	124.60	132.12	128.57	129.10	200.18	192.42	195.42
150	164.10	160.42	161.50	173.92	171.71	171.62	255.24	251.86	256.51
200	197.72	192.79	195.31	212.45	211.23	210.68	303.11	302.74	309.36
250	235.32	227.24	231.81	248.06	247.75	246.81	346.56	349.65	358.13
300	273.75	261.11	268.62	282.92	283.09	281.88	390.04	394.38	404.79
350	313.45	295.22	306.67	315.93	316.51	315.10	430.63	436.15	447.86
400	350.93	328.20	344.30	344.42	345.39	343.80	467.17	474.32	486.18

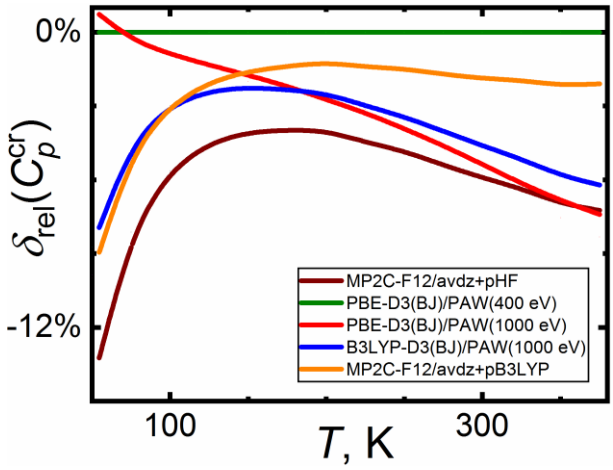

FIGURE S12. Deviation plot of isobaric heat capacities of crystalline [emIm][BF_4] calculated from optimized unit-cell geometries and phonons obtained at the PBE-D3(BJ)/PAW(400 eV) level (reference level 0% here) and unit-cell energy – volume profiles refined at various levels of theory.

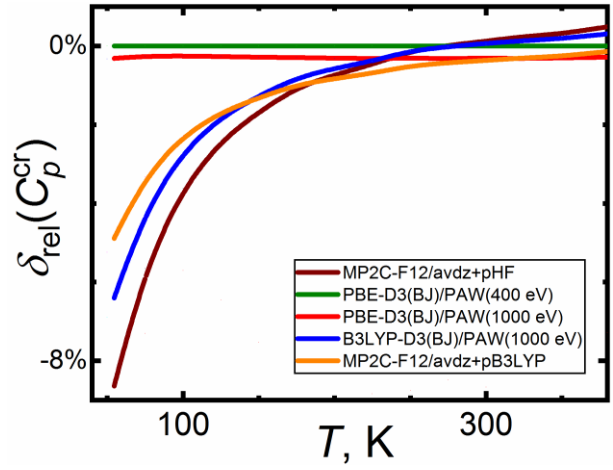

FIGURE S13. Deviation plot of isobaric heat capacities of crystalline [emIm][PF_6] calculated from optimized unit-cell geometries and phonons obtained at PBE-D3(BJ)/PAW(400 eV) level (reference level 0% here) and unit-cell energy – volume profiles refined at various levels of theory.

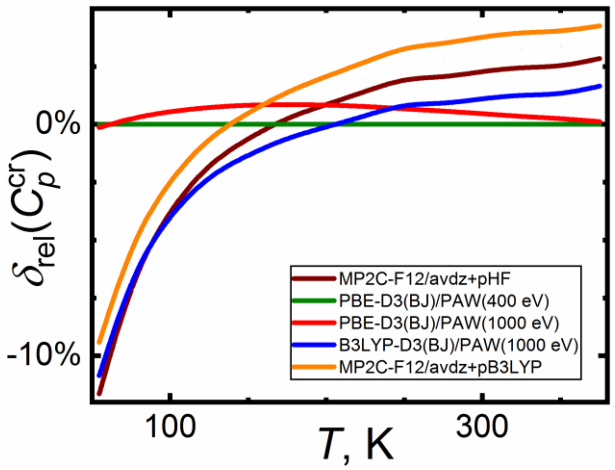

FIGURE S14. Deviation plot of isobaric heat capacities of crystalline [emIm][NTf_2] calculated from optimized unit-cell geometries and phonons obtained at the PBE-D3(BJ)/PAW(400 eV) level and unit-cell energy – volume profiles refined at various levels of theory.

S6. REFERENCES for the SI

(1) Nishida, T.; Tashiro, Y.; Yamamoto, M., Physical and electrochemical properties of 1-alkyl-3-methylimidazolium tetrafluoroborate for electrolyte. *J. Fluorine Chem.* **2003,** *120*, 135-141.

(2) Paulechka, Y. U.; Blokhin, A. V.; Kabo, G. J.; Strechan, A. A., Thermodynamic properties and polymorphism of 1-alkyl-3-methylimidazolium bis(triflamides). *J. Chem. Thermodyn.* **2007,** *39*, 866-877.

(3) Mutch, M. L.; Wilkes, J. S., Thermal Analysis of 1-Ethyl-3-Methylimidazolium Tetrafluoroborate Molten Salt. *Proc. Electrochem. Soc.* **1998,** *1998-11*, 254-260.

(4) D. Holbrey, J.; R. Seddon, K., The phase behaviour of 1-alkyl-3-methylimidazolium tetrafluoroborates; ionic liquids and ionic liquid crystals. *J. Chem. Soc., Dalton Trans.* **1999**, 2133-2140.

(5) Ngo, H. L.; LeCompte, K.; Hargens, L.; McEwen, A. B., Thermal properties of imidazolium ionic liquids. *Thermochim. Acta* **2000,** *357-358*, 97-102.

(6) Noda, A.; Hayamizu, K.; Watanabe, M., Pulsed-Gradient Spin−Echo 1H and 19F NMR Ionic Diffusion Coefficient, Viscosity, and Ionic Conductivity of Non-Chloroaluminate Room-Temperature Ionic Liquids. *J. Phys. Chem. B* **2001,** *105*, 4603-4610.

(7) Valkenburg, M. E. V.; Vaughn, R. L.; Williams, M.; Wilkes, J. S., Thermochemistry of ionic liquid heat-transfer fluids. *Thermochim. Acta* **2005,** *425*, 181-188.

(8) Wachter, P.; Schreiner, C.; Schweiger, H.-G.; Gores, H. J., Determination of phase transition points of ionic liquids by combination of thermal analysis and conductivity measurements at very low heating and cooling rates. *J. Chem. Thermodyn.* **2010,** *42*, 900-903.

(9) Shirota, H.; Mandai, T.; Fukazawa, H.; Kato, T., Comparison between Dicationic and Monocationic Ionic Liquids: Liquid Density, Thermal Properties, Surface Tension, and Shear Viscosity. *J. Chem. Eng. Data* **2011,** *56*, 2453-2459.

(10) Vila, J.; Fernández-Castro, B.; Rilo, E.; Carrete, J.; Domínguez-Pérez, M.; Rodríguez, J. R.; García, M.; Varela, L. M.; Cabeza, O., Liquid–solid–liquid phase transition hysteresis loops in the ionic conductivity of ten imidazolium-based ionic liquids. *Fluid Ph. Equilibria* **2012,** *320*, 1-10.

(11) Wong, D. S. H.; Chen, J. P.; Chang, J. M.; Chou, C. H., Phase equilibria of water and ionic liquids [emim][PF6] and [bmim][PF6]. *Fluid Ph. Equilibria* **2002,** *194-197*, 1089-1095.

(12) Dzyuba, S. V.; Bartsch, R. A., Influence of Structural Variations in 1-Alkyl(aralkyl)-3-Methylimidazolium Hexafluorophosphates and Bis(trifluoromethylsulfonyl)imides on Physical Properties of the Ionic Liquids. *ChemPhysChem* **2002,** *3*, 161-166.

(13) Domańska, U.; Marciniak, A., Solubility of 1-Alkyl-3-methylimidazolium Hexafluorophosphate in Hydrocarbons. *J. Chem. Eng. Data* **2003,** *48*, 451-456.

(14) Sifaoui, H.; Ait-Kaci, A.; Modarressi, A.; Rogalski, M., Solid–liquid equilibria of three binary systems: 1-Ethyl-3-methylimidazolium hexafluorophosphate+2-phenylimidazole, or 4,5-diphenylimidazole or 2,4,5-triphenylimidazole. *Thermochim. Acta* **2007,** *456*, 114-119.

(15) Endo, T.; Masu, H.; Fujii, K.; Morita, T.; Seki, H.; Sen, S.; Nishikawa, K., Determination of Missing Crystal Structures in the 1-Alkyl-3-methylimidazolium Hexafluorophosphate Series: Implications on Structure–Property Relationships. *Cryst. Growth Des.* **2013,** *13*, 5383-5390.

(16) Serra, P. B. P.; Ribeiro, F. M. S.; Rocha, M. A. A.; Fulem, M.; Růžička, K.; Coutinho, J. A. P.; Santos, L. M. N. B. F., Solid-liquid equilibrium and heat capacity trend in the alkylimidazolium PF6 series. *J. Mol. Liq.* **2017,** *248*, 678-687.

(17) Štejfa, V.; Bazyleva, A.; Fulem, M.; Rohlíček, J.; Skořepová, E.; Růžička, K.; Blokhin, A. V., Polymorphism and thermophysical properties of L- and DL-menthol. *J. Chem. Thermodyn.* **2019,** *131*, 524-543.

(18) Ferreira, A. F.; Simões, P. N.; Ferreira, A. G. M., Quaternary phosphonium-based ionic liquids: Thermal stability and heat capacity of the liquid phase. *J. Chem. Thermodyn.* **2012,** *45*, 16-27.
(19) Sanmamed, Y. A.; Navia, P.; González-Salgado, D.; Troncoso, J.; Romaní, L., Pressure and Temperature Dependence of Isobaric Heat Capacity for [Emim][BF4], [Bmim][BF4], [Hmim][BF4], and [Omim][BF4]. *J. Chem. Eng. Data* **2010,** *55*, 600-604.
(20) Gupta, H.; Kataria, J.; Sharma, D.; Sharma, V. K., Topological investigations of molecular interactions in binary ionic liquid mixtures with a common ion: Excess molar volumes, excess isentropic compressibilities, excess molar enthalpies and excess molar heat capacities. *J. Chem. Thermodyn.* **2016,** *103*, 189-205.
(21) Sharma, V. K.; Bhagour, S.; Solanki, S.; Rohilla, A., Thermodynamic Properties of Ternary Mixtures Containing Ionic Liquids and Organic Solvents. *J. Chem. Eng. Data* **2013,** *58*, 1939-1954.
(22) Waliszewski, D.; Stępniak, I.; Piekarski, H.; Lewandowski, A., Heat capacities of ionic liquids and their heats of solution in molecular liquids. *Thermochim. Acta* **2005,** *433*, 149-152.
(23) Yu, Y.-H.; Soriano, A. N.; Li, M.-H., Heat capacities and electrical conductivities of 1-ethyl-3-methylimidazolium-based ionic liquids. *J. Chem. Thermodyn.* **2009,** *41*, 103-108.
(24) Holbrey, J. D.; Reichert, W. M.; Reddy, R. G.; Rogers, R. D., Heat Capacities of Ionic Liquids and Their Applications as Thermal Fluids. In *Ionic Liquids as Green Solvents*, American Chemical Society: 2003; Vol. 856, pp 121-133.
(25) Zaitsau, D. H.; Kabo, G. J.; Strechan, A. A.; Paulechka, Y. U.; Tschersich, A.; Verevkin, S. P.; Heintz, A., Experimental vapor pressures of 1-alkyl-3-methylimidazolium Bis(trifluoromethylsulfonyl)imides and a correlation scheme for estimation of vaporization enthalpies of ionic liquids. *J. Phys. Chem. A* **2006,** *110*, 7303-7306.
(26) Armstrong, J. P.; Hurst, C.; Jones, R. G.; Licence, P.; Lovelock, K. R.; Satterley, C. J.; Villar-Garcia, I. J., Vapourisation of ionic liquids. *Phys Chem Chem Phys* **2007,** *9*, 982-90.
(27) Emel'yanenko, V. N.; Verevkin, S. P.; Heintz, A., The gaseous enthalpy of formation of the ionic liquid 1-butyl-3-methylimidazolium dicyanamide from combustion calorimetry, vapor pressure measurements, and ab initio calculations. *J. Am. Chem. Soc.* **2007,** *129*, 3930-3937.
(28) Tolstoguzov, A. B., Investigation of thermal evaporation of imidazolium-based ionic liquids. *Mass-Spektrom.* **2007,** *4*, 283-288.
(29) Ahrenberg, M.; Brinckmann, M.; Schmelzer, J. W.; Beck, M.; Schmidt, C.; Kessler, O.; Kragl, U.; Verevkin, S. P.; Schick, C., Determination of volatility of ionic liquids at the nanoscale by means of ultra-fast scanning calorimetry. *Phys. Chem. Chem. Phys.* **2014,** *16*, 2971-2980.
(30) Santos, L. M. N. B. F.; Lopes, J. N. C.; Coutinho, J. A. P.; Esperanca, J. M. S. S.; Gomes, L. R.; Marrucho, I. M.; Rebelo, L. P. N., Ionic liquids: First direct determination of their cohesive energy. *J. Am. Chem. Soc.* **2007,** *129*, 284-285.
(31) Luo, H.; Baker, G. A.; Dai, S., Isothermogravimetric Determination of the Enthalpies of Vaporization of 1-Alkyl-3-methylimidazolium Ionic Liquids. *J. Phys. Chem. B* **2008,** *112*, 10077-10081.
(32) Lovelock, K. R.; Deyko, A.; Licence, P.; Jones, R. G., Vaporisation of an ionic liquid near room temperature. *Phys. Chem. Chem. Phys.* **2010,** *12*, 8893-8901.
(33) Wang, C.; Luo, H.; Li, H.; Dai, S., Direct UV-spectroscopic measurement of selected ionic-liquid vapors. *Phys. Chem. Chem. Phys.* **2010,** *12*, 7246-7250.
(34) Rocha, M. A.; Lima, C. F.; Gomes, L. R.; Schroder, B.; Coutinho, J. A.; Marrucho, I. M.; Esperanca, J. M.; Rebelo, L. P.; Shimizu, K.; Lopes, J. N.; Santos, L. M., High-accuracy vapor pressure data of the extended [C(n)C1im][Ntf2] ionic liquid series: trend changes and structural shifts. *J Phys. Chem. B* **2011,** *115*, 10919-10926.

(35) Verevkin, S. P.; Zaitsau, D. H.; Emelyanenko, V. N.; Heintz, A., A new method for the determination of vaporization enthalpies of ionic liquids at low temperatures. *J Phys. Chem. B* **2011,** *115*, 12889-12895.
(36) Zaitsau, D. H.; Fumino, K.; Emel'yanenko, V. N.; Yermalayeu, A. V.; Ludwig, R.; Verevkin, S. P., Structure-property relationships in ionic liquids: a study of the anion dependence in vaporization enthalpies of imidazolium-based ionic liquids. *ChemPhysChem* **2012,** *13*, 1868-1876.
(37) Verevkin, S. P.; Zaitsau, D. H.; Emel'yanenko, V. N.; Yermalayeu, A. V.; Schick, C.; Liu, H.; Maginn, E. J.; Bulut, S.; Krossing, I.; Kalb, R., Making sense of enthalpy of vaporization trends for ionic liquids: new experimental and simulation data show a simple linear relationship and help reconcile previous data. *J Phys. Chem. B* **2013,** *117*, 6473-6486.
(38) Verevkin, S. P.; Ralys, R. V.; Zaitsau, D. H.; Emel'yanenko, V. N.; Schick, C., Express thermo-gravimetric method for the vaporization enthalpies appraisal for very low volatile molecular and ionic compounds. *Thermochim. Acta* **2012,** *538*, 55-62.
(39) Heym, F.; Korth, W.; Etzold, B. J. M.; Kern, C.; Jess, A., Determination of vapor pressure and thermal decomposition using thermogravimetrical analysis. *Thermochim. Acta* **2015,** *622*, 9-17.
(40) Ahrenberg, M.; Beck, M.; Neise, C.; Kessler, O.; Kragl, U.; Verevkin, S. P.; Schick, C., Vapor pressure of ionic liquids at low temperatures from AC-chip-calorimetry. *Phys. Chem. Chem. Phys.* **2016,** *18*, 21381-21390.
(41) Dunaev, A. M.; Motalov, V. B.; Kudin, L. S.; Butman, M. F., Molecular and ionic composition of saturated vapor over EMImNTf 2 ionic liquid. *J. Mol. Liq.* **2016,** *219*, 599-601.
(42) Santos, L. M. N. B. F.; Ferreira, A. I. M. C. L.; Štejfa, V.; Rodrigues, A. S. M. C.; Rocha, M. A. A.; Torres, M. C.; Tavares, F. M. S.; Carpinteiro, F. S., Development of the Knudsen effusion methodology for vapour pressure measurements of low volatile liquids and solids based on a quartz crystal microbalance. *J. Chem. Thermodyn.* **2018,** *126*, 171-186.
(43) Deyko, A.; Lovelock, K. R.; Corfield, J. A.; Taylor, A. W.; Gooden, P. N.; Villar-Garcia, I. J.; Licence, P.; Jones, R. G.; Krasovskiy, V. G.; Chernikova, E. A.; Kustov, L. M., Measuring and predicting Delta(vap)H298 values of ionic liquids. *Phys. Chem. Chem. Phys.* **2009,** *11*, 8544-8555.
(44) King, M. B., Correlation, Prediction and Extrapolation of Vapor-Pressure and Related Thermal Data. *Transactions of the Institution of Chemical Engineers* **1976,** *54*, 54-60.
(45) King, M. B.; Al-Najjar, H., Method for correlating and extending vapor pressure data to lower temperatures using thermal data. Vapor pressure equations for some *n*-alkanes at temperatures below the normal boiling point. *Chemical Engineering Science* **1974,** *29*, 1003-11.
(46) Wexler, A., Vapor-Pressure Formulation for Ice. *Journal of Research of the National Bureau of Standards, Section A: Physics and Chemistry* **1977,** *81*, 5-20.
(47) Ambrose, D.; Davies, R. H., The correlation and estimation of vapor pressures. III. Reference values for low-pressure estimations. *Journal of Chemical Thermodynamics* **1980,** *12*, 871-9.
(48) Mosselman, C.; Van Vugt, W. H.; Vos, H., Exactly integrated Clapeyron equation. Its use to calculate quantities of phase change and to design vapor pressure-temperature relations. *Journal of Chemical & Engineering Data* **1982,** *27*, 246-251.
(49) Rogalski, M., Correlation of vapor pressures of pure substances in homologous series. *Thermochimica Acta* **1985,** *90*, 125-33.
(50) King, M. B.; Mahmud, R. S., A reduced vapour pressure equation for use at low reduced temperatures. *Fluid Phase Equilibria* **1986,** *27*, 309-330.
(51) Craven, R. J. B.; de Reuck, K. M., Development of a vapour pressure equation for methanol. *Fluid Phase Equilibria* **1993,** *89*, 19-29.

(52) Poling, B. E., Vapor pressure prediction and correlation from the triple point to the critical point. *Fluid Phase Equilibria* **1996,** *116*, 102-109.
(53) Varushchenko, R. M.; Pashchenko, L. L.; Druzhinina, A. I.; Abramenkov, A. V.; Pimersin, A. A., Thermodynamics of vaporization of some alkyladamantanes. *Journal of Chemical Thermodynamics* **2001,** *33*, 733-744.
(54) Huber, M. L.; Laesecke, A.; Friend, D. G., Correlation for the Vapor Pressure of Mercury. *Industrial & Engineering Chemistry Research* **2006,** *45*, 7351-7361.
(55) Hogge, J. W.; Giles, N. F.; Knotts, T. A.; Rowley, R. L.; Wilding, W. V., The Riedel vapor pressure correlation and multi-property optimization. *Fluid Phase Equilibria* **2016,** *429*, 149-165.
(56) Hogge, J. W.; Messerly, R.; Giles, N.; Knotts, T.; Rowley, R.; Wilding, W. V., Improving thermodynamic consistency among vapor pressure, heat of vaporization, and liquid and ideal gas isobaric heat capacities through multi-property optimization. *Fluid Phase Equilibria* **2016,** *418*, 37-43.
(57) Fulem, M.; Růžička, K.; Červinka, C.; Bazyleva, A.; Della Gatta, G., Thermodynamic study of alkane-α,ω-diamines – Evidence of odd–even pattern of sublimation properties. *Fluid Phase Equilibria* **2014,** *371*, 93-105.
(58) Fulem, M.; Růžička, K.; Červinka, C.; Rocha, M. A. A.; Santos, L. M. N. B. F.; Berg, R. F., Recommended vapor pressure and thermophysical data for ferrocene. *The Journal of Chemical Thermodynamics* **2013,** *57*, 530-540.
(59) Růžička, K.; Fulem, M.; Červinka, C., Recommended sublimation pressure and enthalpy of benzene. *The Journal of Chemical Thermodynamics* **2014,** *68*, 40-47.
(60) Růžička, K.; Fulem, M.; Růžička, V., Recommended Vapor Pressure of Solid Naphthalene. *Journal of Chemical & Engineering Data* **2005,** *50*, 1956-1970.
(61) Růžička, K.; Majer, V., A simultaneous correlation of vapor pressures and thermal data: application to 1-alkanols. *Fluid Phase Equilibria* **1986,** *28*, 253-264.
(62) Růžička, K.; Majer, V., Simultaneous Treatment of Vapor Pressures and Related Thermal Data Between the Triple and Normal Boiling Temperatures for *n*-Alkanes C_5-C_{20}. *Journal of Physical and Chemical Reference Data* **1994,** *23*, 1-39.
(63) Štejfa, V.; Fulem, M.; Růžička, K.; Červinka, C.; Rocha, M. A. A.; Santos, L. M. N. B. F.; Schröder, B., Thermodynamic study of selected monoterpenes. *Journal of Chemical Thermodynamics* **2013,** *60*, 117-125.
(64) Štejfa, V.; Fulem, M.; Růžička, K.; Matějka, P., Vapor pressures and thermophysical properties of selected hexenols and recommended vapor pressure for hexan-1-ol. *Fluid Phase Equilibria* **2015,** *402*, 18-29.
(65) Štejfa, V.; Fulem, M.; Růžička, K.; Morávek, P., New Static Apparatus for Vapor Pressure Measurements: Reconciled Thermophysical Data for Benzophenone. *Journal of Chemical & Engineering Data* **2016,** *61*, 3627-3639.
(66) M. S. S. Esperança, J.; Canongia Lopes, J. N.; Tariq, M.; Santos, L. M. N. B. F.; Magee, J. W.; Rebelo, L. P. N., Volatility of Aprotic Ionic Liquids — A Review. *J. Chem. Eng. Data* **2010,** *55*, 3-12.
(67) Paulechka, Y. U.; Zaitsau, D. H.; Kabo, G. J.; Strechan, A. A., Vapor pressure and thermal stability of ionic liquid 1-butyl-3- methylimidazolium Bis(trifluoromethylsulfonyl)amide. *Thermochim. Acta* **2005,** *439*, 158-160.